



Communication

Calculation of the band structure and density of localized states of materials of the quasi-binary system $\text{Zn}_3\text{As}_2\text{-Mn}_3\text{As}_2$

V.S. Zakhvalinskii^{a,*}, T.B. Nikulicheva^a, E.A. Pilyuk^a, A.S. Kubankin^a, O.N. Ivanov^b, A. A. Morocho^a

^a Belgorod National Research University, Belgorod, 308015, Russia

^b V.G. Shukhov Belgorod State Technological University, Belgorod, 308012, Russia



ARTICLE INFO

Communicated by: T. Kimura

Keywords:

Magnetic semiconductor
Band structure
Density of localized states
 ZnMn_2As_2
 Zn_3As_2
 Mn_3As_2

ABSTRACT

Investigations of materials of the quasi-binary system $\text{Zn}_3\text{As}_2\text{-Mn}_3\text{As}_2$ have been performed. We present band structure calculations of crystal structures of Zn_3As_2 , Mn_3As_2 and ZnMn_2As_2 within the framework of the density functional theory (DFT) and DFT + U method. The calculations based on first-principles were made using plane waves normalized on pseudopotential with the Quantum Espresso software package. Was obtained, that fundamental gap for Mn_3As_2 and Zn_3As_2 is equal to the optical band gap, while the band gaps for ZnMn_2As_2 was closer. The calculation for Mn_3As_2 and ZnMn_2As_2 by method DFT + U were performed; in these cases, the fundamental band gaps are closer to the optical band gaps, respectively. Considering the series $\text{Zn}_3\text{As}_2 \rightarrow \text{ZnMn}_2\text{As}_2 \rightarrow \text{Mn}_3\text{As}_2$, an increase in the Fermi energy was observed: $E_f = 7.5 \rightarrow 8.98 \rightarrow 12.04$ eV. It was established that the band gap of ZnMn_2As_2 ($E_g = 0.6$ eV) is a direct band gap corresponding to the transition between points $\Gamma \rightarrow \Gamma$ of the Brillouin zone. The E_g value obtained by us is closely known from experiments on optical absorption and the study of the temperature dependence of resistivity with E_g values equal to 0.8 eV and 0.76 eV, respectively. For Mn_3As_2 and ZnMn_2As_2 , splitting is observed in density of states (DOS) between spin up and spin down electrons.

1. Introduction

An increasing interest in diluted magnetic semiconductors (DMSs) is connected with attempts to use these materials in instrumental structures as sources of spin-polarized charge carriers [1]. In addition to comparatively long-studied diluted magnetic semiconductors based on II-VI $\text{Zn}_{1-x}\text{Mn}_x\text{Te}$ and $\text{Cd}_{1-x}\text{Mn}_x\text{Te}$ [2] as well as based on III-V, $\text{In}_{1-x}\text{Mn}_x\text{As}$ and $\text{Ga}_{1-x}\text{Mn}_x\text{As}$ [3] are intensively studied. Recently, a group of DMSs based on II-V compounds are much less known in spite of their extremely attractive magnetic and transport properties; first of all, it should be emphasized that these materials are characterized by a small cation-cation distance among the known DMSs which are not in the II-V group. Small cation-cation distances causes the sp-d (sp-f) exchange interaction between the band carriers and localized magnetic moments of these ions and the d-d (f-f) interaction between the ions themselves, both types of the exchange interactions are much stronger in II-V than in other DMS [4]. The interest in semiconductors of the II-V group and solid solutions based on them increased dramatically after the discovery

of topological properties in the narrow-gap semiconductor Cd_3As_2 [5,6]. The study of ternary and quaternary solid solutions are the subject of considerable current research [7–11], being Zn_3As_2 a representative p-type semiconducting compound of II-V group with space group $P4_2/nmc$ and optical band gap is 1.1 eV [12]. Studies of the structure and magnetic properties of Mn_3As_2 are presented in Refs. [13–15]. The importance of studying the properties of the diluted magnetic semiconductor $(\text{Zn}_{1-x}\text{Mn}_x)_3\text{As}_2$ induced the study of the quasi-binary system $\text{Zn}_3\text{As}_2\text{-Mn}_3\text{As}_2$ [16].

In [16], a phase diagram for the existence of solid solutions $(\text{Zn}_{1-x}\text{Mn}_x)_3\text{As}_2$ and $\text{Zn}_{1\pm x}\text{Mn}_{2\pm x}\text{As}_2$ are presented. The construction of the phase diagram contributed to the technology optimization for producing high quality large single crystals of the ternary magnetic semiconductor ZnMn_2As_2 and solid solutions of DMS $(\text{Zn}_{1-x}\text{Mn}_x)_3\text{As}_2$. This was followed by extensive studies on the new material ZnMn_2As_2 using both x-ray structural and neutron diffraction analysis, as well as the study of the anisotropy of magnetic properties and electrical conductivity of $(\text{Zn}_{1-x}\text{Mn}_x)_3\text{As}_2$ [17–23]. However, it must be emphasized that

* Corresponding author.

E-mail address: zakhvalinskii@bsu.edu.ru (V.S. Zakhvalinskii).

<https://doi.org/10.1016/j.ssc.2021.114237>

Received 13 January 2021; Received in revised form 2 February 2021; Accepted 14 February 2021

Available online 17 February 2021

0038-1098/© 2021 Elsevier Ltd. All rights reserved.

the ternary compounds, mentioned above, and solid solutions based on them are generally poorly (not enough) understood.

The purpose of this paper is to study of quasi-binary system of alloys $\text{Zn}_3\text{As}_2\text{-Mn}_3\text{As}_2$ and to clarify on first-principles the features of the band structure and density of localized states of the ternary magnetic semiconductor ZnMn_2As_2 within the system $\text{Zn}_3\text{As}_2\text{-Mn}_3\text{As}_2$. This can be useful for understanding the anisotropy of the magnetic properties and electrical conductivity of not only ZnMn_2As_2 , but also other solid solutions $(\text{Zn}_{1-x}\text{Mn}_x)_3\text{As}_2$.

2. Crystal structure

Zn_3As_2 is a wide-gap semiconductor with a direct band gap (at the Γ -point of the Brillouin zone). The crystal structure belongs to the tetragonal space group $P4_2/nmc$ (No. 137) and is quite complex. For example, the tetragonal unit cell of $\alpha\text{-Zn}_3\text{As}_2$ contains 160 atoms (96 Zn and 64 As) and can be divided into 16 fluorite cubes provided, where $a = 8.316 \text{ \AA}$ and $c = 11.76 \text{ \AA}$ are the tetragonal lattice constants. Each fluorite cube contains 4 As atoms on a face-centered cubic lattice with a lattice constant $a_0 \cong a/2$ and 6 Zn atoms inside a distorted cubic lattice (the lattice constant $\approx a_0/2$) with two vacancies connected by a diagonal [4].

The Mn_3As_2 semiconductor is a semiconductor with three different modifications. The first modification of Mn_3As_2 (I) is a high-temperature phase with a tendency to twinning. When this phase is cooled, intergrown crystals containing Mn_3As_2 (II) and Mn_5As_4 with very closely related structures are obtained. The third modification of Mn_3As_2 (III) is obtained at low temperatures [24]. Since we were interested in clarifying the features of the band structure of ZnMn_2As_2 at temperatures close to helium, for the comparative series, the third modification of Mn_3As_2 with monoclinic crystal structure and space group $C2/m$ (No. 12) was chosen. We are planning to use data about band structure of ZnMn_2As_2 in our further investigations, for example, studies of the mechanisms of hopping conductivity. The structure of Mn_3As_2 (III), like the other two modifications, can be in the form of close-packed layers formed by arsenic atoms that are broken by manganese clusters around Mn_4 atoms [24].

ZnMn_2As_2 is a layered magnetic semiconductor with a hexagonal space group, which, as was shown in Ref. [17], has an ordered sequence of the doublet of the Mn planes separated by As and Zn planes. As follows from neutron studies [21], the magnetic order does not correspond to the ideal crystal structure, which can be explained by the fact that the Mn planes contain some Zn atoms and vice versa. In Ref. [25], it can be also noticed that ZnMn_2As_2 has a disordered layered structure. This is explained by a chemical disorder in the layered structure, characteristic for the ZnMn_2As_2 structure, related to the coexistence of layers fully occupied by Mn ions, together with mixed Mn/Zn bilayer. These features also make the studies of the ZnMn_2As_2 band structure more attractive and interesting.

3. Experimental details for ZnMn_2As_2

The ZnMn_2As_2 single crystal was obtained by the modified Bridgman method from stoichiometric amounts of Zn_3As_2 and Mn_3As_2 placed in a glass-graphite cup inside an evacuated quartz ampoule. After heating above the melting and synthesis temperature for 10 h, slow cooling was carried out with a rate of 5 K h^{-1} near the melting point 1113 K ; cooling was carried out in the presence of a temperature gradient of 2 K cm^{-1} of the furnace. The spatial symmetry group and unit cell parameters were determined using a Rigaku Ultima IV diffractometer [25].

Absorption spectra were recorded at temperatures of 77 K and 300 K (Fig. 1) for a plane-parallel single crystal plate of ZnMn_2As_2 with a thickness of $d = 1.5 \text{ mm}$; the plane of the plane was the cleavage plane (001) of the space group $P\bar{3}m1$. The evaluation of the width of band gap at the absorption edge gave a value of $E_g \approx 0.8 \text{ eV}$.

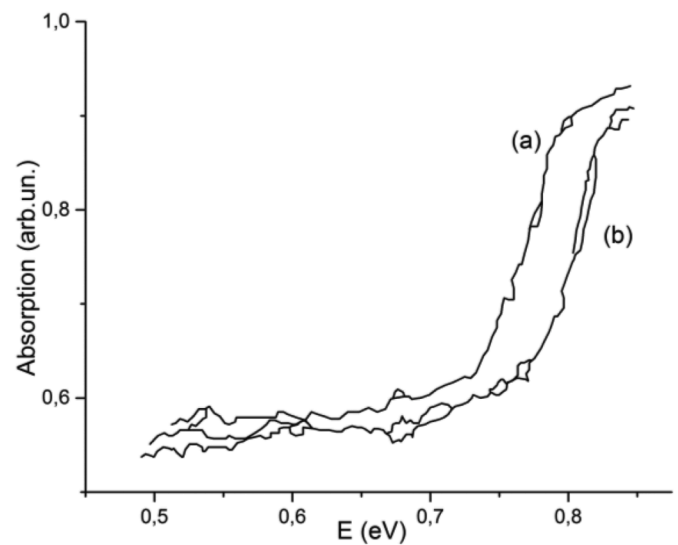


Fig. 1. Absorption spectra of single crystals of ZnMn_2As_2 at temperatures (a) $T = 77 \text{ K}$, (b) $T = 300 \text{ K}$.

The result obtained is in good agreement with the band gap ($E_g = 0.76 \text{ eV}$) determined from the analysis of the temperature dependence of the resistivity.

4. Computational work

First-principles calculations based on density functional theory (DFT) and DFT + U were used for structure of Zn_3As_2 , Mn_3As_2 , ZnMn_2As_2 crystals as implemented in Quantum Espresso software package [26,27]. The calculation involved exchange and correlations according to Perdew–Burke–Ernzerhof (PBE) functional and Ultrasoft Pseudopotential (USPP). The calculated unit cell for Zn_3As_2 , Mn_3As_2 and ZnMn_2As_2 was constructed in the 3D visualization program for structural models VESTA [28]. First Brillouin zone of materials was accomplished using from Monkhorst-Pack method. Marzari-Vanderbilt smearing size was fixed to 0.1 Ry . Geometry optimization of the supercell were performed using variable cell relaxation (vc-relax) calculation as implemented in Quantum Espresso code.

Energy cutoff of 50 Rydberg in a plane-wave basis set was used for calculation. Two different methods were adopted for calculating band structure of Mn_3As_2 : DFT without U value, DFT + U with calculated U. And one method was applied for calculating of ZnMn_2As_2 and Zn_3As_2 : DFT + U with calculated U and DFT without U value, respectively. The calculated Hubbard U was determined using linear response theory.

5. Band structure

The energy band spectra of the compounds under study were calculated at high-symmetry points of the Brillouin zones [29] in their appropriate units, and along lines connecting them.

The results of the calculation of the band structure of Zn_3As_2 , Mn_3As_2 and ZnMn_2As_2 are presented in Fig. 2. The Fermi energy level was chosen as the starting point of the energy scale.

The positions of the calculated bands for Zn_3As_2 and Mn_3As_2 correlate with the structural bands shown in Ref. [30] and the band gap calculated by DFT method was 0.97 eV and 0.18 eV , respectively. Our calculated band gap of Mn_3As_2 using DFT + U method with calculated U is resulted to calculated band gap of 0.0 eV . The values of U was determined through a linear response method which is fully consistent with the definition of the DFT + U Hamiltonian, making this approach for the potential calculations fully ab initio [31], and the U value was 3 eV , what corresponds the data in Ref. [32].

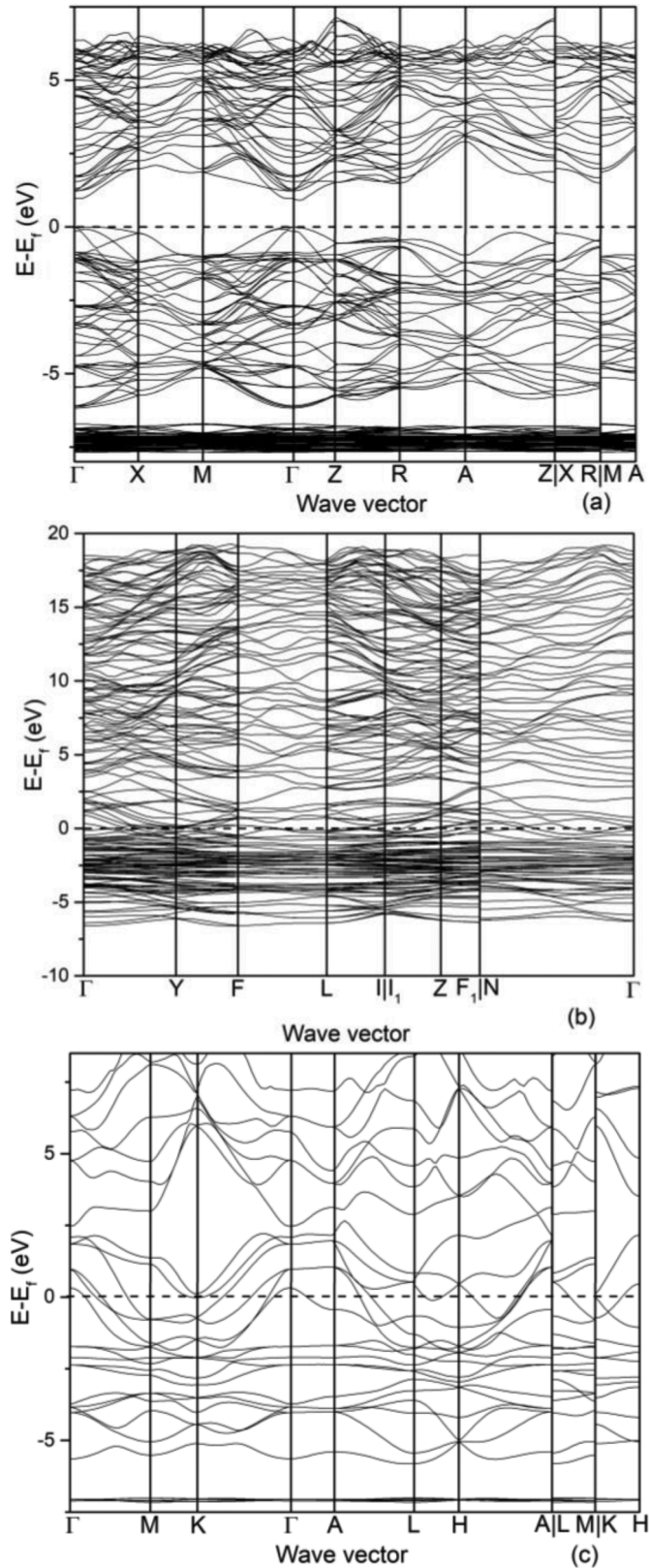


Fig. 2. Band structure of (a) Zn_3As_2 , (b) Mn_3As_2 , (c) ZnMn_2As_2 .

This is results are in good agreement with earlier DFT, DFT + U calculations and experimental data [12,33]. Also in this case of DFT, the “band gap” refers to the fundamental gap [34], and not to the optical band gap [12].

The density functional theory is formulated to calculate the

properties of the ground state.

Although the band structure involves the excitation of electrons into unoccupied states, the Kohn-Sham [35] energies used to solve discrete Fourier transform equations are often interpreted as corresponding to the energy levels of electrons in the solid. The relationship between the Kohn-Sham eigenvalues calculated by discrete Fourier transform method and electron energies is theoretically possible only for the highest occupied electronic state. The Kohn-Sham energy of this state corresponds to the first ionization energy of the material, taking into account the exact exchange-correlation functional. However, for other energies, there are no assumptions that Kohn-Sham eigenvalues will correspond to a physical observable [36]. The fundamental gap energy calculated by us within the framework of the density functional theory (DFT) is not always equal to the optical band gap, being for Zn_3As_2 equal to it, for ZnMn_2As_2 becomes close it, and in the case of Mn_3As_2 it is very different from the optical width of the band gap.

Considering the series $\text{Zn}_3\text{As}_2 \rightarrow \text{ZnMn}_2\text{As}_2 \rightarrow \text{Mn}_3\text{As}_2$, the calculation shows that Fermi energy increases $E_f = 7.5 \rightarrow 8.98 \rightarrow 12.04$ eV. From Fig. 2c, it is possible to determine that ZnMn_2As_2 is a direct narrow-gap semiconductor with band gap (valence band – conduction band) $E_g = 0.6$ eV. The upper part of the valence bands in the energy range $-2.4 \div -1.7$ eV is plane and corresponds to highly localized electronic states. The largest dispersion $E(k)$ takes place in the energy range $-2.5 \div -7.5$ eV, corresponding to the electronic states of the conduction band. The band gap E_g of ZnMn_2As_2 is a direct band gap corresponding to the transition between points $\Gamma \rightarrow \Gamma$ of the Brillouin zone.

The total density of states (DOS) of Zn_3As_2 , Mn_3As_2 , ZnMn_2As_2 is shown in Fig. 3. The density of states shows the contribution of the states of zinc (Zn), manganese (Mn) and arsenic (As), these supports are analyzed by partial density of states (PDOS). Complete DOS of ZnMn_2As_2 is the contribution of the Zn, Mn, and As states, therefore, it is important to understand how electrons are distributed for individual atoms of the system. The Fermi level is in the valence band, indicating a degenerate p-type material that is consistent with the acceptor nature of the Mn.

The total DOS and PDOS of ZnMn_2As_2 are shown in Fig. 4. As follows from the analysis the band gap of ZnMn_2As_2 also is 0.6 eV.

In the DOS for Mn_3As_2 and ZnMn_2As_2 , splitting is observed between spin up and spin down electrons (Fig. 3). The imbalance in the DOS of ZnMn_2As_2 is induced by p-electrons of As and d-electrons of Mn with spin-up and spin-down (Fig. 4), while the DOS distributions for s-electrons with opposite spin-directions are close.

As shown in Figs. 3 and 4 the upper part of the valence bands in the energy range -7.5 to -2.5 eV can be divided into two groups with respect to the separated bands. The first narrow group of the valence bands (-7.5 to -6.8 eV) consists of a single band and is formed mainly by the highly localized d-state of zinc.

6. Conclusion

Using density functional theory (DFT) and DFT + U method, the band structure and the DOS of ZnMn_2As_2 , Zn_3As_2 , and Mn_3As_2 were calculated on the basis of first principles. We analyzed the fundamental energy gap in the framework of the density functional theory (DFT), being equal to the optical band gap in the case of Zn_3As_2 , while for Mn_3As_2 it is very different from the optical width of the band gap. The calculation for Mn_3As_2 and ZnMn_2As_2 by method DFT + U with value Hubbard U equal 3 eV was performed; in this case, the fundamental band gaps is closer to the optical band gap. In case of analysis of ZnMn_2As_2 , the transition $\Gamma \rightarrow \Gamma$ is a direct type transition. The upper valence bands in the energy range $-2.4 \div -1.7$ eV have a relatively weak dependence of energy on the wave vector, which corresponds to highly localized electronic p-states of arsenic. Among the valence electron states with energies in the range of -7.5 to -6.8 eV, the Zn states dominate. For Mn_3As_2 and ZnMn_2As_2 , splitting is observed in DOS between spin up and spin down electrons. The imbalance in the DOS is

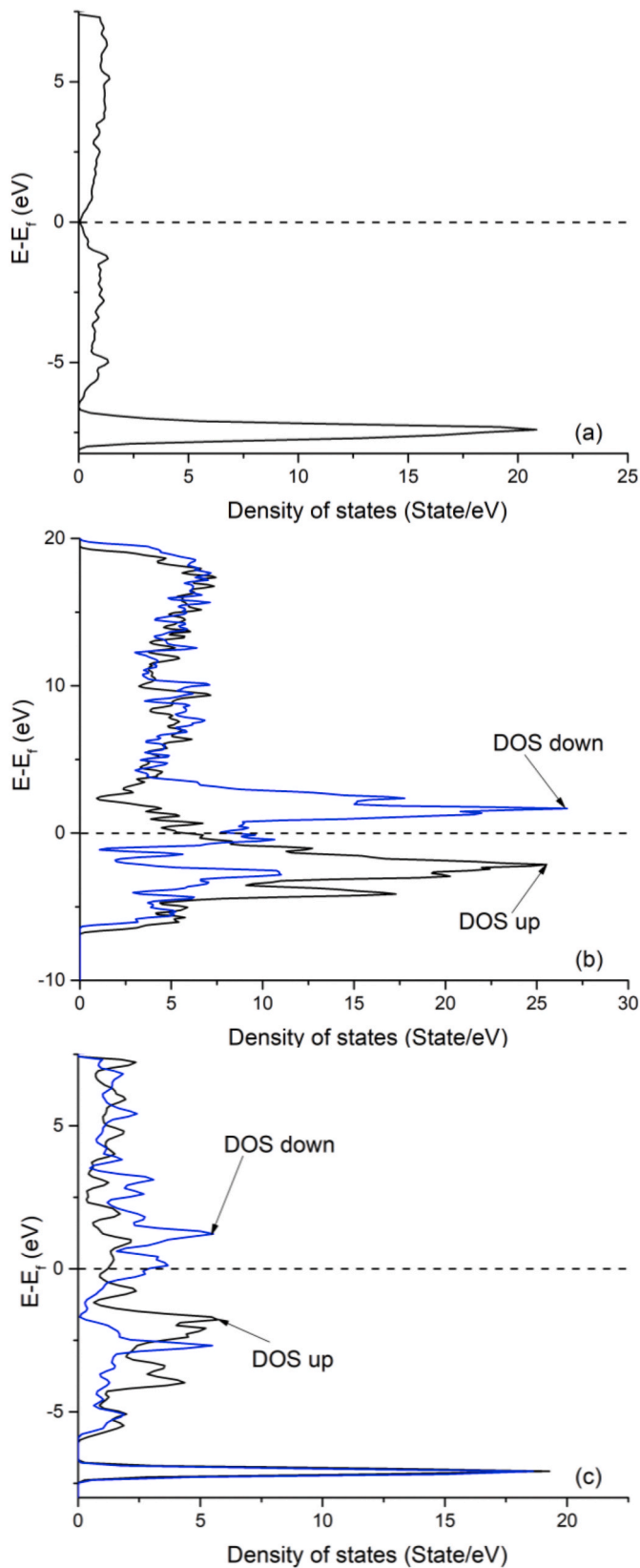


Fig. 3. The density of localized states for (a) Zn_3As_2 , (b) Mn_3As_2 , (c) $ZnMn_2As_2$.

induced by p-electrons of As and d-electrons of Mn with spin-up and spin-down, while the DOS distributions for s-electrons with opposite spin-directions are close.

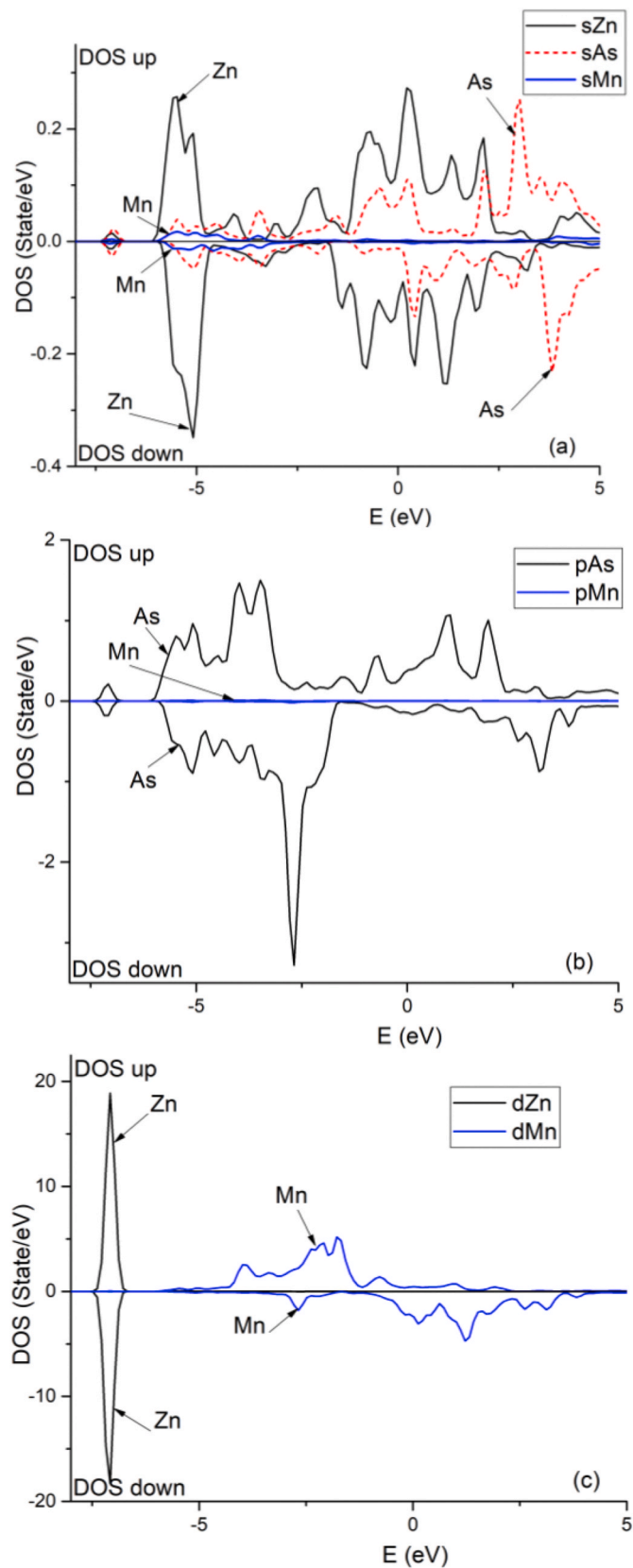


Fig. 4. Partial densities of localized states of $ZnMn_2As_2$.

Author statement

Vasilii S. Zakhvalinskii: Conceptualization, Writing – original draft, Writing – review & editing, Tatyana B. Nikulicheva: Methodology, Writing – original draft, Writing – review & editing, Evgeny A. Pilyuk: Resources, Aleksandr S. Kubankin: Investigation, Oleg N. Ivanov: Writing – original draft, Writing – review & editing, Alexander A. Morocho: Supervision.

Data availability statement

The data that supports the findings of this study are available within the article.

Declaration of competing interest

The authors declare that they have no known competing financial interests or personal relationships that could have appeared to influence the work reported in this paper.

Acknowledgments

A. S. Kubankin thanks a Program of the Ministry of Education and Science of the Russian Federation for higher education establishments for financially supported, Project No. FZWG-2020-0032(2019–1569).

References

- [1] H.S. Kaushik, F.A. Sharma, F.M. Sharma, *Int. J. IT, Eng. Appl. Sci. Res. (IJIEASR)* 3 5 (2014).
- [2] J.K. Furduna, *J. Appl. Phys.* 64 (1988) R29.
- [3] Jungwirth T., JairoSinova, Mašek J., Kučera J. and MacDonald A. H. *Rev. Mod. Phys.* 78 809.
- [4] J. Cisowski, *Phys. Stat. Sol. (b)* 200 (1997) 311.
- [5] Z. Wang, H. Weng, Q. Wu, X. Dai, Z. Fang, *Phys. Rev. B* 88 (2013) 125427.
- [6] Lan-Po He, Shi-Yan Li, *Chin. Phys. B* 25 (8) (2016) 117105.
- [7] V.A. Kulibatchinskii, et al., *Phys. Tekhn. Semicond.* (1991) 252201, in Russian).
- [8] A.V. Lashul, et al., *Phys. Rev. B* 46 (1992) 6251.
- [9] R. Laiho, et al., *J. Phys. Cond. Matt.* 5 (1993) 5113.
- [10] Laiho R, et al., *J. Magn. Magn. Mater.* 140 (1995) 2019.
- [11] O. Ivanov, V. Zakhvalinskii, T. Nikulicheva, M. Yaprincev, S. Ivanichikhin, *Phys. Status Solidi Rapid Res. Lett.* (6) (2018) 1800386.
- [12] J.M. Misiewicz, *Solid State Commun.* 32 (1979) 687.
- [13] M.H. Möller, W. Jeitschko, *Z. Kristallogr.* 204 (1993) 77.
- [14] M.F. Hagedorn, W. Jeitschko, *J. Solid State Chem.* 113 (1994) 257.
- [15] L.H. Dietrich, W. Jeitschko, M.H. Möller, *Z. Kristallogr.* 190 (1990) 259.
- [16] V.S. Zakhvalinskii, R.Iu Lialikova, A.N. Nateprov, *Izv. Acad. of Sci. Mold. Ser. Fys. and Tekhn.* 187 (1991).
- [17] A.A. Dvorkin, I.A. Verin, V.S. Zakhvalinskii, *Sov. Phys. Crystallogr.* 36 (1991) 785.
- [18] I. Mirebeau, SuardÉ, M. Hennion, M.T. Fernandez-Diaz, A. Daoud-Aladine, A. Nateprov, *J. Magn. Magn. Mater.* 175 (1997) 290.
- [19] M. von Ortenberg, I. Laue, A. Nateprov, J. Vanacken, I. Mirebeau, *Physica B* 201 (1994) 57.
- [20] A. Nateprov, I. Tomak, J. Heimann, J. Cisowski, I. Mirebeau, *J. Magn. Magn. Mater.* 172 (1997) 193.
- [21] I. Laue, et al., *Phys. Status Solidi* 185 (1994) 245.
- [22] L. Konopko, et al., *Cryst. Respir. Technol.* 31 (1996) 659.
- [23] E. Suard, I. Mirebeau, A. Daoud-Aladine, NateprovA, *Phys. B Condens. Matter* 241–243 (1997) 739.
- [24] M.F. Hagedorn, W. Jeitschko, *J. Solid State Chem.* 113 (2) (1994) 257.
- [25] O. Ivanov, V. Zakhvalinskii, T. Nikulicheva, M. Yaprincev, *Mater. Res. Exp.* 6 (2019) 105908.
- [26] P. Giannozzi, et al., *J. Phys. Condens. Matter* 21 (2009) 395502.
- [27] P. Giannozzi, et al., *J. Phys. Condens. Matter* 29 (2017) 465901.
- [28] K. Momma, F. Izumi, *J. Appl. Crystallogr.* 41 (3) (2008) 653.
- [29] W. Setyawan, S. Curtarolo, *Comput. Mater. Sci.* 49 (2010) 299.
- [30] Anubhav Jain, et al., *APL Mater.* 1 (2013), 011002.
- [31] V.L. Campo, M. Cococcioni, *J. Phys. Condens. Matter* 22 (2010), 055602.
- [32] V. Stevanovic, S. Lany, X. Zhang, A. Zunger, *Phys. Rev. B* 85 (2012) 115104.
- [33] M. Kaur, K. Kabra, R. Kumar, B.K. Sharma, G. Sharma, *J. Alloys Compd.* 709 (2017) 179.
- [34] E.N. Brothers, A.F. Izmaylov, J.O. Normand, V. Barone, G.E. Scuseria, *J. Chem. Phys.* 129 (2008), 011102.
- [35] P. Erhart, A. Klein, R.G. Egdell, K. Albe, *Phys. Rev. B* 75 (15) (2007) 153205.
- [36] R. Godby, M. Schluter, L.J. Sham, *Phys. Rev.* (1988) B3710159.